

**Linear Relationship Between Weighted-Average Madelung Constants and Density Functional Theory Energies for MgO Nanotubes**

Journal:	<i>The Journal of Physical Chemistry</i>
Manuscript ID:	jp-2012-08041d.R1
Manuscript Type:	Article
Date Submitted by the Author:	08-Nov-2012
Complete List of Authors:	Baker, Mark; University of Guelph, Department of Chemistry and Biochemistry Baker, Arthur; Queens College CUNY, Chemistry Belanger, Jane; University of Guelph, Mathematics and Statistics Hanusa, Christopher; Queens Colleg CUNY, Mathematics Michaels, Alana; CUNY,Queens College, Chemistry and Biochemistry

SCHOLARONE™  
Manuscripts

1  
2  
3 OCTOBER 30 2012  
4  
5  
6  
7

8 **Linear Relationship between Weighted-average Madelung Constants**  
9 **and Density Functional Theory Energies for MgO Nanotubes**  
10

11  
12  
13  
14  
15  
16 Mark D. Baker,<sup>\*1</sup> A. David Baker<sup>2</sup>, Jane Belanger,<sup>3</sup> Christopher R. H. Hanusa,<sup>4</sup>  
17 and Alana Michaels<sup>2</sup>  
18  
19

20  
21 1. Department of Chemistry, University of Guelph, Guelph, Ontario N1G 2W1, Canada.  
22

23 2. Department of Chemistry and Biochemistry, Queens College, City University of New York,  
24 Flushing NY 11367, USA.  
25

26  
27 3. Department of Mathematics and Statistics, University of Guelph, Guelph, Ontario N1G 2W1,  
28 Canada.  
29

30 4. Department of Mathematics, Queens College, City University of New York, Flushing NY  
31 11367, USA.  
32  
33  
34  
35  
36  
37  
38  
39  
40  
41  
42  
43  
44  
45  
46  
47  
48  
49  
50  
51  
52  
53  
54  
55  
56  
57  
58  
59  
60

**ABSTRACT**

For systems containing large numbers of ions, calculations using Density Functional Theory (DFT) are often impractical because of the amount of time needed to perform the computations. In this paper, we show that weighted-average Madelung constants of MgO nanotubes correlate in an essentially perfectly linear way with cohesive energies determined by DFT. We discuss this correlation in terms of the relationship between lattice energies and cohesive energies. Through this linear correlation, Madelung constants are used to predict cohesive energies and average ion charges of nanostructures containing up to 3940 ions. Cohesive energies of MgO nanotubes are shown to converge to a value lower than those of bulk MgO. Using the slopes of the DFT versus Madelung constant plots the average charges on the ions in the nanotubes are determined. For nanotubes containing the same number of ions, the relative stability of longer tubes versus disc-like structures is discussed.

**KEYWORDS:** Nanotubes, Density Functional Theory, Magnesium Oxide, Madelung Constant

## INTRODUCTION

The structures and relative stabilities of ionic nanotubes are important in both a fundamental and applied sense. The quest to understand their structures and relative stabilities has stimulated a large research effort in synthetic and theoretical chemistry circles<sup>1-8</sup>. Recently a DFT study of the relative stabilities of alkali halide nanotubes has appeared in this journal<sup>9</sup>. In this paper, we show how energy calculations for MgO nanotubes can be performed many times faster using weighted-average Madelung constant calculations.

Bonding in bulk ionic materials such as MgO and NaCl occurs predominantly via electrostatic coulombic interactions. Indeed, lattice and cohesive energies can be accurately modeled using Born-Mayer-like potential functions. However, the bonding occurring within nanostructures of these materials can be less straightforward because covalent interactions can become significant<sup>5</sup>. Quantum mechanical calculations have been adopted to attack this issue, with DFT (Density Functional Theory) methods being the most popular. This route is computationally challenging and so far calculations have been limited to clusters containing fewer than 500 ions.

Assessing the ionic contribution to the bonding in nanostructures is less challenging. Electrostatic potentials can be determined via coulomb sums combined with the Madelung Constant<sup>10-12</sup>. We have developed algorithms that allow the rapid determination of Madelung Constants (and thus electrostatic energies) for even large arrays of ions<sup>11</sup>. For finite structures, ions in different environments are present, and have different Madelung Constants. The algorithms we have developed can generate all these values, and they relate to the electric potential associated with each ion, and as such are useful for investigating surface properties.

1  
2  
3 Also the weighted average Madelung Constant,  $MC(wa)$ , of all the individual ions in a structure  
4  
5 can be determined, and is proportional to the coulombic contribution to the overall cohesive  
6  
7 energy of a cluster of ions. Indeed, it is implemented in the Born-Mayer equation (equation 5,  
8  
9 vide infra).

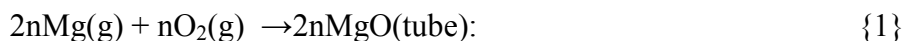
10  
11  
12 Our methods circumvent the need for partial charges required by the Ewald<sup>13</sup> and Evjen<sup>14</sup>  
13  
14 approaches to the calculation of Madelung Constants and are, in contrast to these methods,  
15  
16 applicable to neutral and finite nanostructures. The  $MC(wa)$  values determined in this paper are  
17  
18 correlated with our DFT calculations on MgO nanotubes of various shapes and sizes. As shown  
19  
20 in Table 3, the  $MC(wa)$  values are almost perfectly linearly correlated with our DFT calculations  
21  
22 on MgO nanotubes of various shapes and sizes. It is important to note that the  $MC(wa)$  values for  
23  
24 the nanotubes studied here are significantly different from the bulk value and also do not  
25  
26 converge to the bulk value commonly used in lattice energy calculations.  
27  
28  
29  
30

### 31 32 **COMPUTATIONAL METHODS**

33  
34 Weighted-average Madelung Constants were computed via coulomb sum  
35  
36 algorithms within a particular structure<sup>11-13</sup>. The usual assumptions of point charges with a  
37  
38 closest near-neighbor distance of unity were followed<sup>11</sup>. The determinations, even for particles  
39  
40 with 100,000 ions, run in a few seconds on a desktop computer using Fortran 77 algorithms and  
41  
42 double precision arithmetic. DFT calculations were undertaken in the Gaussian 09 suite<sup>15</sup> using  
43  
44 Microsoft Windows and Macintosh OS X platforms. Energy minimizations were effected using a  
45  
46 6-311G(d) basis set and a B3LYP functional. All nanotube cohesive energies in this paper are  
47  
48 given in eV. The formalism used to describe the nanotubes is illustrated in Fig 1. Each tube is  
49  
50 identified by the number of ions in the polygon base and the number of layers of the stacked  
51  
52 polygons in the nanotubes. For example a nanotube with 8 ions in the base (4 Mg and 4 O) and 5  
53  
54  
55  
56  
57  
58  
59  
60

1  
2  
3 repeat units (see Fig 1b) is designated as a 5L8 tube. So 5L8 explicitly means five layers of eight  
4 ions. Collectively tubes will be referred to by their base polygon sizes so the 5L8 tube is a  
5 member of the L8 family of nanotubes. Data are reported for two general types of nanotubes; 1.  
6 those with an "ideal" structure where each layer of the nanotube is a perfectly regular polygon  
7 and 2. those which have an optimized geometry produced by the DFT routine. In this paper these  
8 will be distinguished by the descriptors ideal and optimized.  
9  
10  
11  
12  
13  
14  
15  
16

17 The cohesive binding energy  $E(\text{coh})$  of the MgO nanotubes was determined by  
18 considering the net chemical reaction to form the structures<sup>5</sup>:  
19  
20  
21



23 where  $n$  is the number of ion pairs in the nanotube, and  $2nE(\text{coh})$  is the energy change  
24 associated with this reaction.  
25  
26  
27

28 thus;

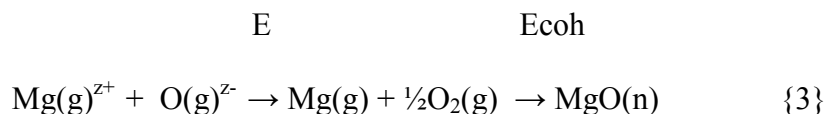
$$29 \quad E(\text{coh}) = 1/n[ E(\text{tube}) - n\{E_0(\text{Mg})\} - n/2 \{E_0(\text{O}_2)\}] \quad \{2\}$$

30  
31  
32  
33  
34  
35  
36  
37  $E(\text{tube})$  is the total energy of the nanotube determined from DFT methods and  $E_0(\text{Mg})$   
38 and  $E_0(\text{O}_2)$  are the total electronic energies of the Mg gas phase atom and the triplet ground state  
39 of  $\text{O}_2$ . These two energies thus serve as an arbitrary reference. Using a 6-311G(d) basis set and a  
40 B3LYP functional the energies of Mg and  $\text{O}_2$  were -200.0930924 and -150.3647909 a.u.  
41 respectively. Geometry optimizations were launched with an initial guess geometry of an ideal  
42 nanotube with a near neighbor distance of  $2\text{\AA}$ . In all DFT geometry optimizations a subsequent  
43 frequency calculation was performed in order to confirm that a true minimum was reached. No  
44 negative frequencies were observed. The vibrational analyses will be presented in a future  
45 publication. DFT optimizations of ideal structures where each layer was maintained as a regular  
46  
47  
48  
49  
50  
51  
52  
53  
54  
55  
56  
57  
58  
59  
60

1  
2  
3 polygon (all bond lengths and angles were equal) was performed as follows. Mathematica was  
4 used to calculate the coordinates of each ion as the bond length was varied in each nanotube. The  
5 families of coordinates were then fed into the Gaussian DFT routine, from which the bond length  
6 that yielded the optimum energy was recorded. Data analysis and fitting procedures were  
7 conducted using the Origin 7 suite (Origin Lab, Northampton MA). Depictions of the structures  
8 were generated using Chemcraft Software (<http://www.chemcraftprog.com>). The average near-  
9 neighbor distance in the optimized structures was determined using the distance matrix produced  
10 by the Gaussian 09 software.  
11  
12  
13  
14  
15  
16  
17  
18  
19  
20  
21

## 22 RESULTS AND DISCUSSION

23  
24 Figure 2 shows plots of  $E(\text{coh})$  (see equation 2 above) versus the weighted-average Madelung  
25 Constant ( $MC(\text{wa})$ ) for L4,L6,L8,L10 and L20 nanotubes with two to nine layers. The length of  
26 the tubes increases from left to right in all cases. Complete data are also assembled in Tables 1-3.  
27 Note that these values are not fitted values but are explicitly given from the DFT calculations and  
28 the values are given in Table 3. There is an almost perfect linear correlation (Correlation  
29 coefficient  $R$  values are given in Table 3) between  $E(\text{coh})$  and the  $MC(\text{wa})$  which warrants  
30 further discussion. Although the correlation between bulk lattice energies and  $MC$ 's is well  
31 known, the correlation in this paper between DFT energies of nanotubes and their weighted-  
32 average  $MC$  has not been reported before. This can be framed by considering a step-wise  
33 thermodynamic route from the gas phase ions to a  $\text{MgO}$  nanotube ( $\text{MgO}(n)$ ):  
34  
35  
36  
37  
38  
39  
40  
41  
42  
43  
44  
45  
46  
47



51 The overall process is, by definition, the lattice energy  $E(\text{lat})$  of  $\text{MgO}(n)$  and so:  
52  
53

$$54 \qquad \qquad \qquad E(\text{lat}) = E + E(\text{coh}) \qquad \{4\}$$

Moreover the lattice energy can be determined via the Born-Mayer equation:

$$E(\text{lat}) = MC(\text{wa}) (z^+ \cdot z^-) e^2/4\pi\epsilon_0 r + b \exp^{-ar} \quad \{5\}$$

Where  $r$  is the average-shortest Mg-O bond distance,  $b$  is a compressibility constant and  $a$  is a constant.<sup>14</sup>

Combining equations {4} and {5} and rearranging gives:

$$E(\text{coh}) = MC(\text{wa}) (z^+ \cdot z^-) e^2/4\pi\epsilon_0 r + b e^{-ar} - E \quad \{6\}$$

Thus a plot of  $E(\text{coh})$  vs.  $MC(\text{wa})$  will be linear with a slope of  $(z^+ \cdot z^-) e^2/4\pi\epsilon_0 r$  and intercept  $b \exp^{-ar} - E$ . It is important to note that this analysis uses the Madelung Constant for the ideal array of ions (for which the MC can only be used as it demands a perfect periodic array) and applies it to an optimized (non-perfect array). This is reasonable because the thermodynamic scheme in equation {3} can be modified by an additional step:  $\text{MgO}(n) \rightarrow \text{MgO}(n,\text{opt})$  where the latter is the optimized nanotube. The energy associated with the step is independent of the Madelung Constant but will contribute to the intercept. This is discussed later.

We now return to the data assembled in Tables 2 and 3, and Fig. 2. First we consider the slope of the plots for the optimized structure. From equation {6} above and the average value of  $r$  from the DFT calculations (see Computational Methods above and Table 2) the average charge on magnesium and oxygen can be determined. In all cases, the charges are substantially less than the classic  $\pm 2$  used for the bulk material. Here, the charge varies from 1.307 for the 2L4 tube to 1.112 for the 2L20 tube. These values are in general agreement with several other studies<sup>16-18</sup>. For example the 4L4 and 4L6 tubes values of 1.318 and 1.219 are in agreement with the data of Bilabegovich<sup>16</sup> (1.39,1.4), Roberts and Johnston<sup>17</sup> (1 to 1.3 and 1.1 to 1.5), Calvo<sup>18</sup> (1.22.no value given) and Chen et al.<sup>5</sup> (1.08,1.13). The data of Bilabegovich and Chen suggest that the average charge on the ions increases both with tube length and diameter (increasing number of

ions in the base of the tube). Our data agree with these trends as the tubes lengthen but are converse to their results as the tubes widen. Our data show that the charges are smaller for the same number of layers for increasingly wider nanotubes. (see Table 3). This is entirely consistent with the correlation between the DFT (cohesive energies) and the weighted- average Madelung Constants. The correlations shown in Figure 2 indicate that  $z^2/4\pi\epsilon_0 r$  (the slope) is constant for any family of nanotubes. Thus as  $r$  decreases with increasing nanotube diameter so must the effective charge also decrease. The data presented here are thus completely self-consistent.

It is interesting to compare the relative slopes and cohesive energies of the  $E(\text{coh})$  vs.  $MC(\text{wa})$  plots for the idealized structures, with those of the optimized structures which in all cases assumed a slightly barrel-like shape (see later). In all cases the geometry optimization produced the most stable nanotube. Nonetheless, the plots are not parallel. An example is shown in Fig.3 for the L10 and L20 families of tubes. It appears that for each family of tubes, there is a critical point where the ideal structure should be more stable. This is in fact not the case as we now discuss. We first consider the L4, L6, L8, and L10 tubes. The plots (mathematically) cross at  $MC(\text{wa})$  values of 13.762, 1.747, 1.672 and 1.678 respectively. However, none of these values are physically reasonable. The maximum possible value for all of these lies in the range 1.595 (for the L4 tubes) to 1.621 (for the L20 tubes; see below for exact values). In other words, as with the bulk crystals the attainable Madelung Constants converge to a limiting value. In the case of the L4 tubes, the value exceeds that of the bulk material (1.747). In the other three cases the value of the MC is unattainable (i.e, is beyond the convergence value). No matter how long the tube is, the  $MC(\text{wa})$  cannot reach these values. For the L4, L6, L8, L10 and L20 tubes the  $MC(\text{wa})$  converges to 1.595, 1.608, 1.612, 1.613 and 1.621 respectively. This indicates that in the case of these tubes the barrel-like geometry will always be adopted. However in the case of the

1  
2  
3 L20 nanotube family, the crossing point is at  $MC(wa) = 1.615$ . This value can be achieved and  
4  
5 occurs for a nanotube containing 7,500 layers. Thus tubes with more layers than this will adopt  
6  
7 the ideal structure. The average Mg-O distance is approximately  $2\text{\AA}$  and so the critical tube  
8  
9 length is about 1.5 microns. Beyond this, ideal tubes will form, but because the  $MC(wa)$  has  
10  
11 converged and remains unchanged and less than the bulk value, all tubes longer than 1.5 microns  
12  
13 will melt at the same temperature but lower than the bulk material.  
14  
15

16  
17 We now consider the relative stability of the optimized L4, L6, L8, L10 and L20 families  
18  
19 containing the same number of ions. In Table 2 the cohesive energies and  $MC(wa)$  are given for  
20  
21 the small nanotubes that were used in DFT calculations (largest nanotube contains 90 ions). It is  
22  
23 clear from the data that the most stable conformation of nanotubes containing the same number  
24  
25 of ions cannot be predicted merely from the  $MC(wa)$ . For example in the case of the 6L4  
26  
27 ( $E_{coh} = -5.259$  eV,  $MC = 1.548$ ) , 4L6 ( $E_{coh} = -5.422$  eV,  $MC(wa) = 1.546$ ) and 3L8 ( $E_{coh}$   
28  
29  $= -5.356$ ,  $MC(wa) = 1.532$ ). In this case for the 24-ion nanotubes the 4L6 is more stable even  
30  
31 though the  $MC(wa)$  for the 6L4 is larger. However this can be reversed. For example; 4L5  
32  
33 ( $E_{coh} = -5.145$  eV,  $MC(wa) = 1.539$ ) and 2L10 ( $E_{coh} = -5.046$ ,  $MC(wa) = 1.497$ ).  
34  
35 Nonetheless, the  $E_{coh}$  vs.  $MC$  correlation can be used to determine the  $E_{coh}$  for nanotubes  
36  
37 containing large nanotubes composed of too many ions to allow for DFT calculations in any  
38  
39 reasonable time-frame. The cohesive energy is however easily determined from the slope and  
40  
41 intercept of the  $E_{coh}$  vs.  $MC(wa)$  plot and the value of  $MC(wa)$  for any size tube.  
42  
43  
44  
45  
46  
47

48 We now compare the relative stabilities of L4, L6, L8, L10 and L20 (optimized) tubes  
49  
50 containing 3840, 1920, 960, 480 and 120 ions. The results are assembled in Table 4. In the case of  
51  
52 the 3840-ion containing tubes the 192L20 (widest) tube is the most stable ( $E_{coh} = -6.171$  eV).  
53  
54 In concert, the results for the 1920-ion containing tubes indicate the widest of the tubes studied  
55  
56  
57  
58  
59  
60

1  
2  
3 (96L20) is the most stable. This behavior is however not observed for tubes containing  
4  
5 960,480,240 and 120 ions. In the 960 ion nanotubes, the 96L10 tube is more stable. Note also  
6  
7 that the MC(wa) is larger than the 48L20 nanotube. For the 480-ion tubes once again the L10 is  
8  
9 the most stable (48L10:  $E(\text{coh}) = -6.122$  eV, MC (wa) = 1.608). The L10 nanotube is also more  
10  
11 stable in the case of 240 ions, but for 120 ions the L8 tube is most stable ( $E(\text{coh}) = -5.987$  eV  
12  
13 versus  $-5.982$  eV for the 12L10 tube). It is certainly not intuitively obvious that this would be the  
14  
15 case.  
16  
17  
18

19  
20 Finally we consider the magnitude of the barrel-like distortion of the ideal structures.  
21  
22 Above we discussed how the additional energy associated with the stabilization from an ideal  
23  
24 structure to the optimized geometry would contribute to the intercept of the  $E(\text{coh})$  vs. MC plot.  
25  
26 One would therefore expect that the largest difference in intercept ( $\Delta I$ ) between the ideal and  
27  
28 optimized structure would result in the largest distortion. This is indeed the case as shown in  
29  
30 Figure 4 and Table 3. The distortion is visually the largest for the 6L20 ( $\Delta I = 2.797$  eV) in  
31  
32 contrast to 9L10 ( $\Delta I = 1.367$  eV), 9L8 ( $\Delta I = 1.291$  eV), 9L6 ( $\Delta I = 1.117$  eV) and 9L4 ( $\Delta I =$   
33  
34  $10.121$  eV).  
35  
36  
37  
38

39  
40 Finally, we return to discuss the covalent bonding that may be significant for these  
41  
42 nanotubes. The partial charges exhibited (vide supra; Table 3) which are markedly different from  
43  
44 those exhibited by the bulk crystals indicate incomplete charge transfer and possibly some  
45  
46 covalency. The degree of covalency in ionic nanotubes is certainly a matter of interest. It is  
47  
48 tempting to conclude that the near perfect correlations we have found between cohesive energies  
49  
50 and Madelung Constants (which relate to electrostatic interactions only) suggest that electrostatic  
51  
52 interactions are dominant. However, there have been a number of earlier studies that have  
53  
54 suggested that both types of bonding are present. For example, Calvo et al.<sup>18</sup> have suggested that  
55  
56  
57  
58  
59  
60

1  
2  
3 for cubic clusters of MgO it appears that there are significant electrostatic and covalent  
4 contributions to the bonding. In that scenario the explanation for the near perfect correlations  
5  
6 would be more complex than invoking a dominant amount of ionic bonding. Furthermore, for the  
7  
8 nanotubes we have studied the charges are significantly different from the classic bulk value of  
9  
10 plus and minus 2 for the magnesium and oxide ions. Perhaps of interest is that as the tubes are  
11  
12 enlarged (cross sectional width and length) the number of surface ions increases. Indeed unlike  
13  
14 cubic clusters no bulk ions with six-fold coordination are present. In addition if you compare the  
15  
16  $n$ th and  $(n+1)$ th members of a series, then the change in lattice energy would equal the change in  
17  
18 cohesive energy if no terms other than coulombic were playing a role. In fact they are not equal  
19  
20 showing that the correlations we describe are not solely due to electrostatic effects. It has been  
21  
22 suggested that the charge on ions in clusters increases with the gradual formation of higher  
23  
24 coordination number ions The issues of charge and covalency are intertwined, and we are now  
25  
26 engaging in additional studies to better quantify these.  
27  
28  
29  
30  
31  
32  
33  
34  
35  
36  
37  
38  
39  
40  
41

## 42 SUMMARY AND CONCLUSIONS

43  
44 In this paper we have demonstrated that the weighted average Madelung Constants for  
45  
46 MgO nanotubes show an essentially perfect linear correlation with the cohesive binding energies.  
47  
48 The slope of these plots can usefully be employed to assess the average charges of the ions in the  
49  
50 structures. Moreover, the combination of intercept and slopes of the correlations can be used to  
51  
52 predict the relative stabilities of large nanotubes.  
53  
54

55  
56 The principal new physical insights that are a direct result of the work described above are:  
57  
58  
59  
60

- MgO nanotubes have smaller Madelung Constants than a bulk crystal no matter how long the tube is. This means they will melt at lower temperatures than the parent bulk material.
- The most stable nanotube within a family possessing the same number of ions is not necessarily the longest or widest.
- The critical length of L20 nanotube is about 1.5 microns. (7,500 layers). At this size, an idealized tube (undistorted) is the most stable conformation and beyond this length the **melting** point will be constant, but lower than the bulk value. Currently this transition can only be determined by the use of Madelung Constants.

## ACKNOWLEDGMENTS

ADB acknowledges the receipt of PSC-CUNY grant 69597-00 38 which supported this research.

CRHH gratefully acknowledges support from PSC-CUNY grant PSCOOC-40-124. MDB

acknowledges funding from The Natural Sciences and Engineering Research Council of Canada.

We gratefully acknowledge Dr. Uwe Oehler (University of Guelph) for his immense patience and help in designing the programs used in this work.

## REFERENCES

1. Yang, Q.; Sha, J.; Wang, L.; Wang, Y.; Ma, Y.; Wang, J.; Yang, D. *Nanotechnology* **2004**, *15*, 1004-1008.
2. Beck, K. M.; Henyk, M.; Wang, C.; Treisanutto, P. E.; Sushko P.V.; Hess, W. P.; Shluger, A. L. *Phys. Rev. B* **2006**, *74* 045404-1 - 045404-5.
3. Ziemann, P. J.; Castleman, A.W. *J. Chem. Phys.* **1991**, *94*, 718-728.
4. Federov, P. P; Tkachenko, E. A.; Kuznetsov, S. V.; Voronov, V.V.; Lavrishchev, S. V. *Inorg. Mater.* **2007**, *43* 502-504
5. Chen, L.; Xu, C; Zhang, C. C.; Zhou, T.. *Int. J. Quant. Chem.* **2009**, *109*, 349-356.

- 1
  - 2
  - 3
  - 4
  - 5
  - 6
  - 7
  - 8
  - 9
  - 10
  - 11
  - 12
  - 13
  - 14
  - 15
  - 16
  - 17
  - 18
  - 19
  - 20
  - 21
  - 22
  - 23
  - 24
  - 25
  - 26
  - 27
  - 28
  - 29
  - 30
  - 31
  - 32
  - 33
  - 34
  - 35
  - 36
  - 37
  - 38
  - 39
  - 40
  - 41
  - 42
  - 43
  - 44
  - 45
  - 46
  - 47
  - 48
  - 49
  - 50
  - 51
  - 52
  - 53
  - 54
  - 55
  - 56
  - 57
  - 58
  - 59
  - 60
6. Nahtigal, I. G.; Svishchev, I. M. *J. Supercrit. Fluids* **2009**, *50* 169-175.
7. Dong, R.; Chen, X.; Wang, X.; Lei, W. *J. Chem. Phys.* **2008**, *129*, 044705-1 -044705-3.
8. Puente, de la E.; Aguado, A.; Ayuela, A.; Lopez, J.M.; *Phys. Rev. B.* **1997**, *56*, 7607-7614
9. Fernandez-Lima, F.A.; Vernika-Henkes, A.; da Silvera, E.F. *J. Phys. Chem. C*, **2012**, *116*, 4965-4969
10. Madelung, E. *Phys. Zs.* **1918**, *19* 524—533.
11. Baker, A.D.; Baker, M. D. *J. Phys. Chem C.* **2009**, *113*, 14793-14797.
12. Baker, M. D.; Baker, A. D. *J. Chem. Ed.* **2010**, *87*, 280-284.
13. Ewald, P. *Ann. Phys.* **1921**, *369*, 253—287.
14. Evjen, H.M. *Phys. Rev.* **1932**, *39*, 675—687.
15. Gaussian 09, Revision A.02, Frisch, M. J.; Trucks, G. W.; Schlegel, H. B.; Scuseria, G. E.; Robb, M. A.; Cheeseman, J. R.; Scalmani, G.; Barone, V.; Mennucci, B.; Petersson, G. A.; et al.
16. Bilabegovic, G. *Phys. Rev. B* **2004**, *70*, 04507-1 – 04507-6
17. Roberts, C.; Johnston, R.L. *Phys. Chem. Chem. Phys.* **2001**, *3*, 5024 – 5034
18. Calvo, F. *Phys. Rev. B* **2002**, *67*, 161403-1 – 161403-4

## TABLES

**TABLE 1:** Weighted average Madelung Constants for MgO nanotubes.\* Note that DFT calculations were only performed on tubes up to nine layers because of time constraints. (See Table 3)

Layers	L4	L6	L8	L10	L20
2	1.45602993	1.48388742	1.4931747	1.49720758	1.502686197
3	1.50119476	1.52477823	1.53240578	1.53564226	1.540011424
4	1.524971175	1.54566259	1.55226574	1.55503675	1.558761597
5	1.53898554	1.55813184	1.56415703	1.56665266	1.57000792
6	1.54840068	1.56645696	1.5720882	1.57440456	1.577505674
7	1.55510003	1.5724003	1.5777526	1.57993566	1.5828612
8	1.56013515	1.5768588	1.58200108	1.58409086	1.58687785
9	1.56404646	1.58032616	1.5853054	1.587315	1.5900019
10	1.56717797	1.58310019	1.5879488	1.5890201	1.59250115
12	1.57187356	1.58726116	1.59191408	1.593821	1.59625002
14	1.57522765	1.59023328	1.59474636	1.59764606	1.59892788
16	1.5774324	1.59246237	1.59687058	1.59861874	1.60093611
18	1.57969981	1.59419611	1.59852275	1.60032295	1.60249813
20	1.58126508	1.5955831	1.59984448	1.60152432	1.60374776

\* Madelung Constant for bulk MgO is 1.74756459

**TABLE 2:** Data for Optimized MgO Nanotubes : Top to bottom in each cell: Cohesive Energies (eV), average MgO near-neighbor distances (Å) and average ion charges (atomic units).

Layers	L4	L6	L8	L10	L20
2	-4.096 1.969 1.307	-4.748 1.954 1.201	-4.972 1.948 1.157	-5.046 1.945 1.143	-5.151 1.940 1.112
3	-4.867 1.997 1.316	-5.201 1.978 1.216	-5.358 1.972 1.164	-5.421 1.970 1.150	-5.494 1.966 1.120
4	-4.974 2.004 1.318	-5.422 1.988 1.219	-5.556 1.982 1.167	-5.601 1.980 1.153	-5.567 1.976 1.122
5	-5.145 2.009 1.320	-5.554 1.993 1.221	-5.674 1.988 1.169	-5.721 1.986 1.155	-5.769 1.982 1.124
6	-5.259 2.012 1.321	-5.641 1.997 1.222	-5.752 1.992 1.171	-5.794 1.990 1.156	-5.837 1.987 1.125
7	-5.341 2.014 1.321	-5.705 1.999 1.223	-5.808 1.994 1.171	-5.847 1.992 1.156	
8	-5.403 2.015 1.322	-5.752 2.001 1.223	-5.850 1.996 1.171	-5.887 1.994 1.157	
9	-5.454 2.016 1.322	-5.789 2.002 1.224	-5.883 1.998 1.172	-5.917 1.996 1.157	

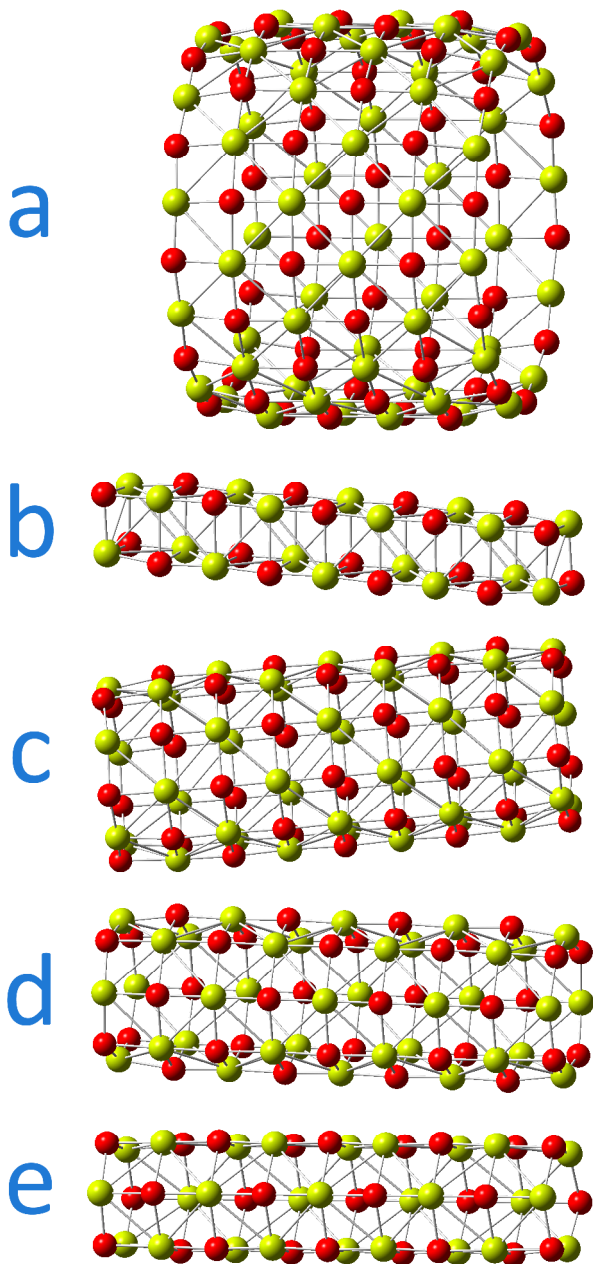
**TABLE 3:** Graphical data for  $E_{\text{coh}}$  vs MC(wa) data: Top to bottom in each cell:  
optimized structure, ideal structure

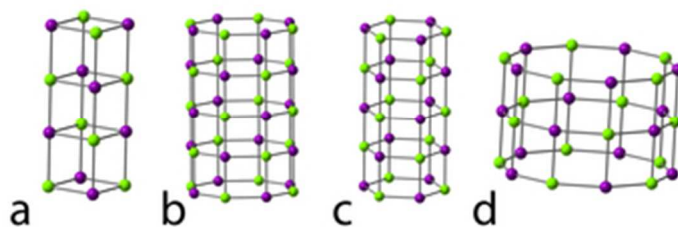
Nanotube	R	intercept /eV	slope/ eV
L4	0.99984	14.07638	-12.48856
	0.99997	14.19735	-12.49735
L6	0.99991	10.89361	- 10.46594
	0.99993	12.0109	-11.21745
L8	0.99997	9.72185	- 9.74868
	0.99987	11.01278	-11.01278
L10	0.99999	9.13679	- 9.38393
	0.99981	10.50395	-10.30948
L20	1	8.6352	-9.17455
	0.99991	11.43204	-10.90631

**TABLE 4:** Weighted –Average Madelung Constants and Predicted Cohesive Energies for MgO nanotubes containing the same number of ions. Top to bottom in each cell: MC, E(coh) in eV. The most stable nanotube is highlighted.

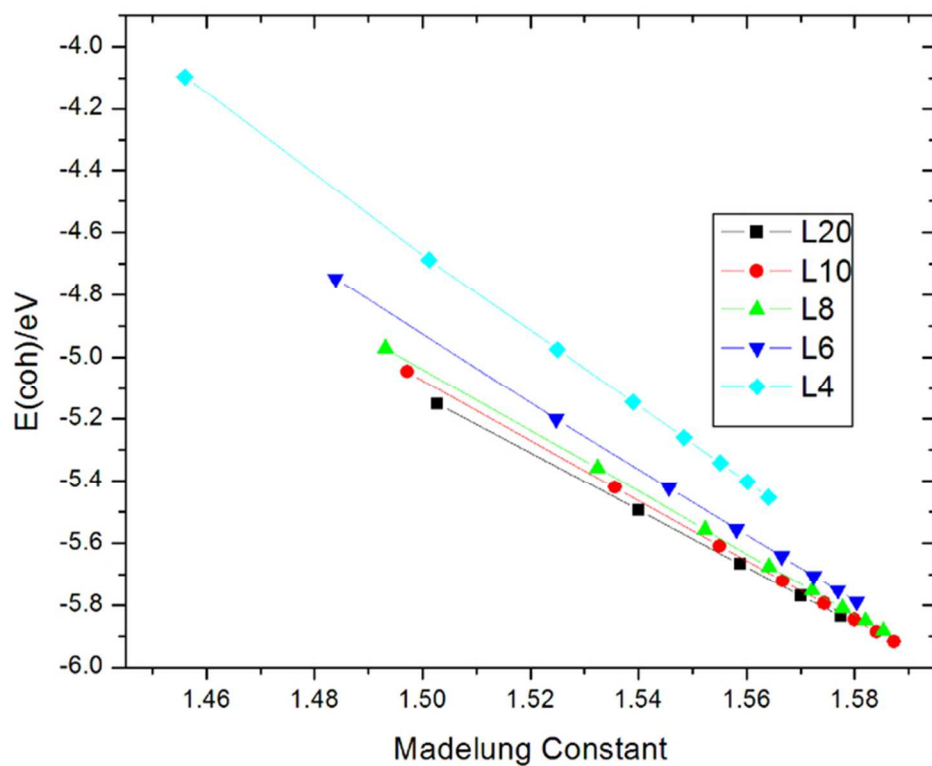
number of ions	L4	L6	L8	L10	L20
3840	1.595	1.608	1.611	1.613	<b>1.614</b>
	-5.844	-6.086	-6.139	-6.163	<b>-6.171</b>
1920	1.595	1.607	1.611	1.612	<b>1.613</b>
	-5.840	-6.081	-6.134	-6.157	<b>-6.160</b>
960	1.594	1.606	1.610	<b>1.611</b>	1.610
	-5.833	-6.073	-6.124	<b>-6.146</b>	-6.139
480	1.593	1.605	1.608	<b>1.608</b>	1.606
	-5.818	-6.056	-6.105	<b>-6.122</b>	-6.095
240	1.591	1.602	1.604	<b>1.604</b>	1.596
	-5.788	-6.023	-6.066	<b>-6.075</b>	-6.010
120	1.586	1.596	<b>1.596</b>	1.594	1.578
	-5.730	-5.958	<b>-5.987</b>	-5.982	-5.838

## TOC Graphic

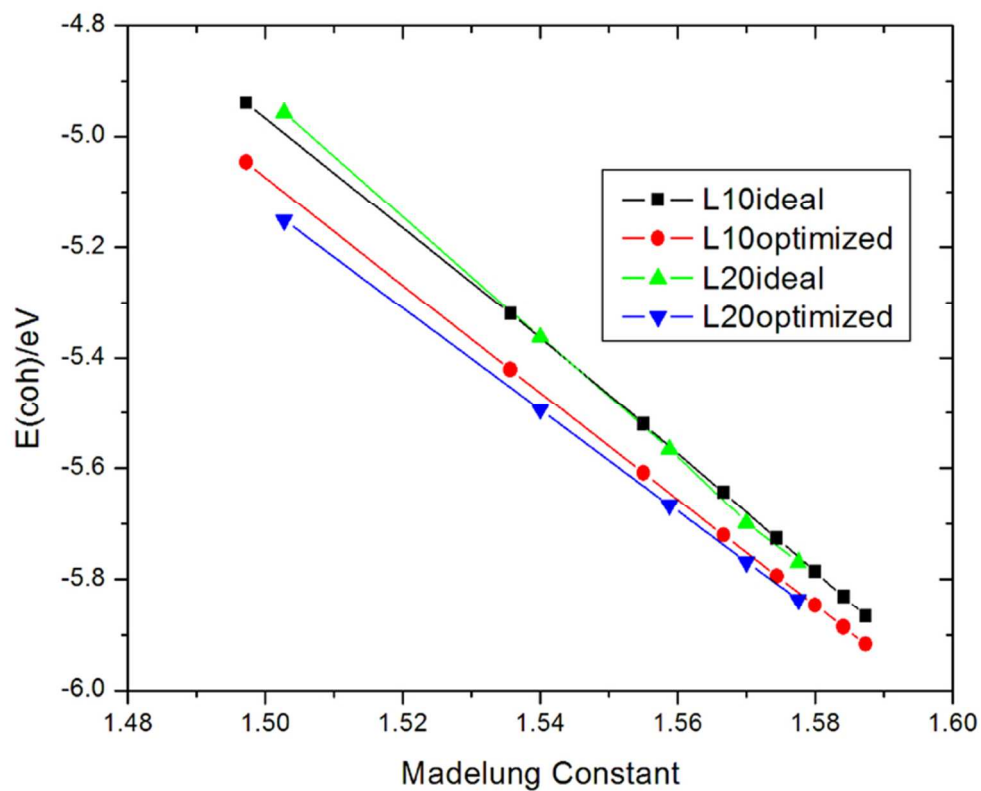




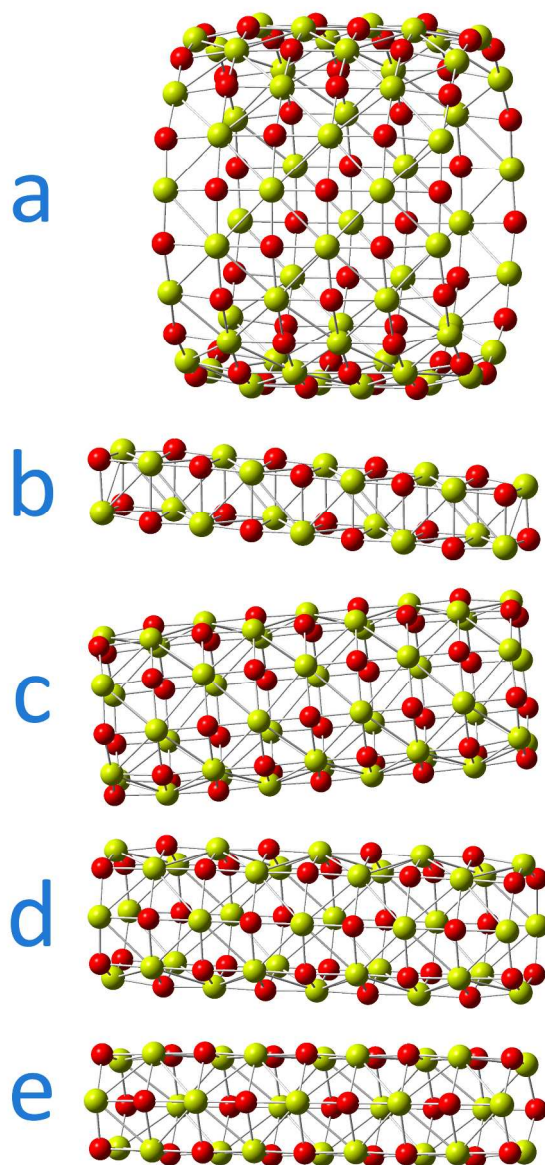
Structure designations of MgO nanotubes. a. 4L4. b. 5L8 c.5L6. d.3L10. Tube axes are vertical  
30x11mm (300 x 300 DPI)



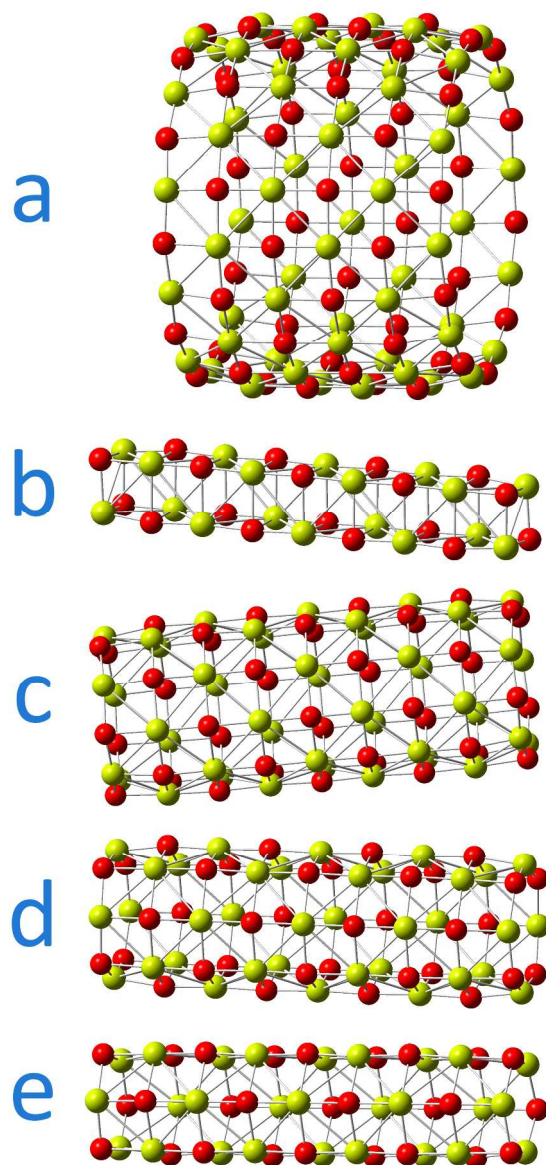
E(coh) vs. Madelung Constant for optimized MgO nanotubes. The length of the tubes increases from left to right in all cases.  
64x50mm (300 x 300 DPI)



A comparison of the  $E(\text{coh})$  vs. Madelung Constant plots for ideal and optimized nanotubes of the L10 and L20 families.  
66x53mm (300 x 300 DPI)



Optimized structures of L4, L6, L8, L10 and L20 nanotubes. In each case the longest tube that was optimized is shown. a) 6L20, b) 4L9, c) 9L10 d) 9L9, e) 9L6. Note that the barrel-like distortion is more evident for the L20 nanotube. Note that unlike Figure 1, the tube axes are horizontal.  
172x361mm (300 x 300 DPI)



172x361mm (300 x 300 DPI)